SOLAR FLARES: THE GRADUAL PHASE

ZDENĚK ŠVESTKA
SRON Laboratory for Space Research Utrecht, The Netherlands

Abstract. One has to distinguish between two kinds of the gradual phase of flares: (1) a gradual phase during which no energy is released so that we see only cooling after the impulsive phase (*a confined flare*), and (2) a gradual phase during which energy release continues (*a dynamic flare*).

The simplest case of (1) is a *single-loop flare* which might provide an excellent opportunity for the study of cooling processes in coronal loops. But most confined flares are far more complicated: they may consist of sets of unresolved elementary loops, of conglomerates of loops, or they form arcades the components of which may be excited sequentially. Accelerated particles as well as hot and cold plasma can be ejected from the flare site (coronal 'tongues', flaring arches, sprays, bright and dark surges) and these ejecta may cool more slowly than the source flare itself.

However, the most important flares on the Sun are flares of type (2) in which a magnetic field opening is followed by subsequent reconnection of fieldlines that may continue for many hours after the impulsive phase. Therefore, the main attention in this review is paid to the gradual phase of this category of *long-decay* flares. The following items are discussed in particular: The wide energy range of dynamic flares: from eruptions of quiescent filaments to most powerful cosmic-ray flares. Energy release at the reconnection site and modelling of the reconnection process. The 'post-flare' loops: evidence for reconnection; observations at different wavelengths; energy deposit in the chromosphere, chromospheric ablation, and velocity fields; loops in emission; shrinking loops; magnetic modelling. The gradual phase in X-rays and on radio waves. Post-flare X-ray arches: observations, interpretation, and modelling; relation to metric radio events and mass ejections, multiple-ribbon flares and anomalous events, hybrid events, possible relations between confined and dynamic flares.

1. Introduction

One has to distinguish between two different kinds of the gradual phase of flares: there are flares, in which all the energy is released within a few seconds, or tens of seconds during the impulsive phase, and the gradual phase is simply the cooling of the heated flare plasma; but there are other flares, in which the release of energy continues during the gradual phase, in extreme cases for many hours. For simplicity, following the classification first proposed by Pallavicini, Serio, and Vaiana (1977), one can call the first class of events 'compact' or 'confined' flares and the second class 'two-ribbon', 'long-decay', or 'dynamic' flares. There are, of course, many hybrids of these two classes of flares, as we will discuss later on.

2. Confined Flares

The most simple case of a confined flare is a single-loop flare. Some people believe that such flares do not exist at all, because the basic mechanism of all flares is an interaction of loops (e.g., cf. Machado, 1987). On the other hand, theorists love single-loop flares, because they can be handled theoretically in a simple way (cf., e.g., Van Hoven, 1981). Well, as it seems, such flares do exist, but are probably very rare. As an example the

Solar Physics **121** (1989) 399–417.

reader is referred to a flare observed by the AS&E group on Skylab at 23:04 UT on 1 September, 1973 (Petrasso *et al.*, 1975): a young active region consisted of three loops; the central one flared for about seven minutes while the general configuration of the active region apparently did not change (cf. Petrasso and Krieger, 1976).

Most flares, however, are more complicated: more loops are involved in the brightening, or an arcade of loops is seen, in which the individual loops may brighten sequentially, one after another. Even in the Petrasso's flare one cannot be quite sure that it was just one simple loop that brightened: it may be a conglomerate of elementary loops, parallel or twisted, the structure of which was below the resolving power of 4 arc sec of the AS&E soft X-ray telescope.

2.1. Single-loop flares

But let us suppose that in some cases we see a single-loop flare. Then, under the assumption of cooling through classical conduction and radiation, one can compute basic physical characteristics of the flaring loop. As an example, Pallavicini *et al.* (1983) computed the expected time evolution of maximum temperature and density in a single-loop compact flare, predicted the corresponding spectral line intensities, and compared them with available observations. The agreement with observations was found better for high-temperature lines than for low-temperature lines, which indicates that the cooling process somewhat deviates from expectations: some flares have decay times much longer than predicted. The authors suggested that this happened simply because the flaring structure in reality was not a single loop, but a conglomerate of shorter and longer loops: the shorter loops evolve more rapidly, the longer loops cool slower.

This may well be true, but Antiochos and Sturrock (1978) have shown that also the process of cooling need not be as simple as these and other authors had assumed. The hot thermal condensation near the top of the loop can cause continuing chromospheric evaporation even after the impulsive phase is over. The evaporation reduces the conductive heat flux into the chromosphere. Acton *et al.* (1982) applied these considerations to a compact flare observed by the SMM and actually found an evidence of continuous evaporation and improved agreement with observations: according to their results, about 7×10^{37} chromospheric atoms evaporated into the loop, and 3×10^{37} electrons were needed to produce the observed soft X-ray emission.

In a later paper, Antiochos and Sturrock (1982) proposed a model in which rapid radiative cooling at the flare loop base creates strong pressure gradients which, in turn, generate large downward flows. Hence, most of the thermal energy of the coronal flare plasma may be lost by mass motions rather than by conduction or radiation. In that case, the differential emission measure has a strong temperature dependence, and Schmahl, Kundu, and Erskine (1986), when comparing microwave and X-ray data, really found such a case in several flares. It seems that this 'condensation cooling' may be important after the evaporation phase is over and before radiation fully dominates the energy losses.

Even simple flares may greatly differ in their characteristics. Some flares studied by

Schmahl, Kundu, and Erskine (1986) showed an unusually high ratio between microwave and X-ray fluxes. On the other hand, Tsuneta (1987) describes compact flares in which this ratio is unusually low. He calls these flaring structures 'hot thermal flares' and suggests that density in these flares is abnormally high: in flares of low-density particle acceleration occurs first, and only after evaporation, i.e., density enhancement, the mode of energy release gradually changes into the plasma heating; in hot thermal flares the density is so high that the accelerated particles are thermalized since the flare onset.

2.2. Associated Phenomena

Thus both the heating and cooling processes may widely differ even in the most simple confined flares. In addition to it, there are secondary phenomena that accompany some of these flares and eventually may become more impressive than the source flare itself: the cooling of these secondary features may be slower, and thus their lifetime longer than that of the confined flare. I will present here three examples.

2.2.1. *Coronal 'Tongues'*

First, I want to draw attention to De Jager's 'Queens' Flare'. Figures in De Jager *et al.* (1983) show how energetic electrons streamed from a low-lying confined limb flare into a previously existing magnetic loop system, thus forming a less bright but long-lived tongue above the limb. At 10 keV this tongue was 35 000 km long and could be seen for 90 min, while the lifetime of the source flare was less than 15 min. At 0.7 keV the tongue lived still longer. Its cooling was very slow and its structure must have been highly filamentary, with filling factor perhaps as low as 0.01.

2.2.2. *Flaring Arches*

As a second example, I refer to a recent paper by Martin and Švestka (1988), where we described the phenomenon of 'flaring arches'. In the brightest event we saw, a small confined subflare appeared at the primary footpoint. Within a few seconds streams of electrons enhanced the secondary footpoint at a distance of 57 000 km. The whole arch between the footpoints brightened in > 16 keV X-rays within one minute while the Hα flow needed 8 min to reach the secondary footpoint. In Hα the flow continued long after the subflare at the primary footpoint decayed. Another flaring arch we studied was 260 000 km long – I suppose Sara Martin will say more about this phenomenon in her review that follows. Similar events were also reported by Mouradian, Martres, and Soru-Escaut (1983), and by Rust, Simnett, and Smith (1985).

The fact that the Hα flow is seen in emission implies that the density of the cool (about 10 000 K) gas that fills the arch must be rather high: $\geq 10^{12}$ cm^{-3}. This follows from empirical considerations made years ago by Zirin, and from computations made recently by Fontenla and Machado (in Švestka *et al.*, 1987) or Heinzel and Karlický (1987). On the other hand, the X-ray energy spectrum requires temperatures in excess of 20 million Kelvin (or particle streams simulating such high temperatures). Thus the flaring arches are a mixture of a huge quantity of a cold dense material and hot, less dense plasma injected into preexisting coronal loops from confined flares or subflares.

2.2.3. *Bright Surges*

Sotirovski, Simon, and Rust (1986) observed a somewhat similar event: a bright surge, seen both in Hα emission and in X-rays, with the Hα flow delayed by about 5 min behind the X-ray enhancement. The authors also conclude that the surge was composed of both hot, X-ray emitting plasma and cold absorbing material. We have also seen such events when comparing Big Bear Observatory and HXIS data.

All this shows that even the 'simple' phenomenon of a compact or confined flare may be sometimes very complex and not at all easy to interpret and understand. It seems reasonable to consider the tongue, the arch, or the surge or spray, which often survive longer than the flare source itself, for a significant component of the gradual phase of these flaring events.

3. Dynamic Flares

However, the most important flares on the Sun belong to the other kind: flares, in which the energy release continues during the gradual phase. There is a wide energetic spectrum of these phenomena: from eruptions of quiescent filaments, the so called 'disparition brusque', when no Hα flare is observed, to powerful two-ribbon flares of X importance in X-rays and 4B importance in Hα, with a set of 'post'-flare loops connecting the ribbons. The common characteristic of all these events is soft X-ray brightening of the corona above the neutral line that lasts for many hours. Therefore, Kahler (1977) invented for them the name 'Long-Decay Events'.

Kopp and Pneuman (1976) suggested that these flares start with the opening of magnetic field lines and subsequent field line reconnection gives rise to the 'post'-flare loops. The resulting configuration is essentially the same that was earlier proposed by Sturrock (1968): energy release at the top of the loops and heating of Hα bright ribbons at their footpoints. Kopp and Pneuman added a dynamic development to this old Sturrock model: the plasma begins to flow upwards after the fieldline opening so that the gas pressure decreases, magnetic pressure prevails, and the process of fieldline reconnection sets in: first very fast, later with decreasing speed, while the neutral point is rising up. Therefore, these events are also called 'dynamic flares'.

3.1. Kopp and Pneuman Model

While most people presently accept this model and some have contributed to its improvement, others are still skeptical, though nobody has been able so far to suggest anything better. Therefore, allow me to spend some time on arguments that support the Kopp–Pneuman interpretation.

3.1.1. *Energy Release during the Gradual Phase*

I think that there is now little doubt that in these flares energy continues to be released for a long time after the end of the impulsive phase. There are many observations that provide evidence for it – let me mention just a few (some more will become obvious in the following sections):

(1) Twenty years ago Bruzek (1969), during his stay at Sacramento Peak, discovered that the Hα post-flare loops do not expand, but that the growth of the loop prominence system is due to the generation of higher and higher loops while the lower ones fade. Each individual loop starts as a rapid brightening of a knot above existing loops which grows and eventually flows downward along the magnetic field lines.

(2) While this process can be usually followed in Hα for a relatively short period of one-and-half hour or less, X-ray observations show the growth of these loops for many more hours. On 29 July, 1973, for example, Skylab observed the growth of loops in a dynamic flare for 11 hours at least. The speed of growth, originally some 50 km s^{-1}, decreased then to 0.5 km s^{-1}, but the altitude of the X-ray loops was still increasing. Calculations showed that cooling time of the loops seen in X-rays was much shorter than the duration of the whole event; thus also in X-rays new loops had to be sequentially formed (Moore *et al.*, 1980).

(3) In another dynamic flare observed by Skylab, MacCombie and Rust (1979) observed that for at least 8 hours bright X-ray flare loops were hotter at the tops than along the legs which implies that continuous heating must have been taking place at the loop tops.

(4) When studying X-ray images of the dynamic flare of 6 November, 1980, Švestka *et al.* (1987) have found a clear dependence of the loop top altitude on the temperature corresponding to the different images (Figure 1(a)): 20×10^6 K for HXIS and Fe XXV, 10×10^6 K for Si XIII, 4×10^6 K for Mg XI, 2×10^6 K for O VIII, and 10000 K for the Hα line. A plausible explanation is that we see here the newly formed loops in the hottest lines, and older loops at lower altitudes during the process of their cooling.

(5) Doyle and Raymond (1984) analyzed a major dynamic flare, taking spectra of the loops for more than 3 hours in the range 400–1335 Å. They found the total energy losses, integrated over the flare decay, far greater than the thermal energy content of the flare plasma at the beginning of observations, shortly after the flare maximum phase.

3.1.2. *Source of the Energy Release*

Thus the fact that energy is released during the gradual phase of dynamic flares has been established beyond any doubt. Another question is what kind of process causes this energy release and loop excitation. Kopp and Pneuman claim that it is reconnection of fieldlines that opened at the onset of the flare. The reconnection starts low in the corona, where the magnetic pressure is greatest, proceeds upwards, and gradually slows down in the upper layers. Still it can, slowly but persistently, continue for hours, as observed.

Really, I do not know any other interpretation that could explain the observed growth of the loop system. Which other process could release energy for 10 or more hours high in the corona, rising upwards with speeds of a few hundred meters per second? If there is no reconnection, i.e., if there are preexisting loops which are gradually excited by a rising agent, what is this agent, moving upwards for ten hours with a speed eventually as low as half-a-kilometer per second? Thus, really, the Kopp–Pneuman interpretation seems to be the only plausible explanation of the observed growth of loops in the dynamic flares.

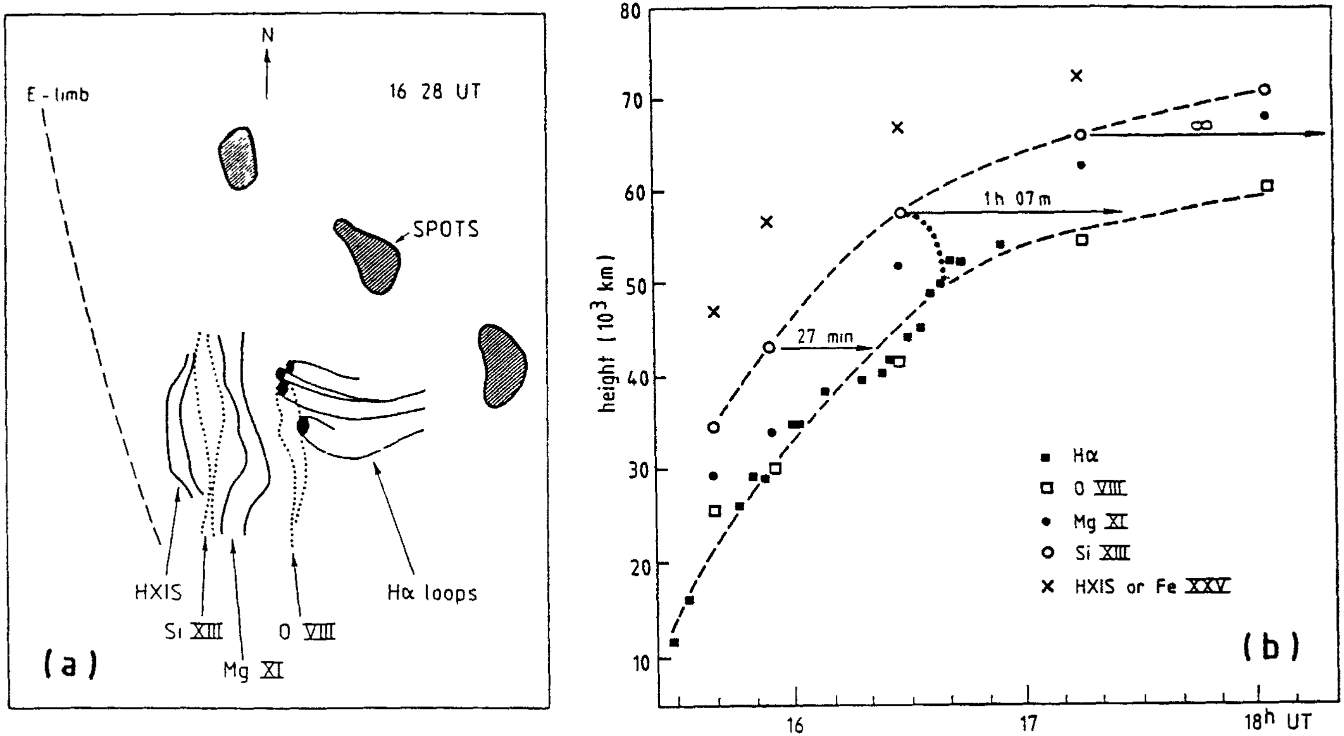

Fig. 1. (a) Positions of the tops of the loops in the dynamic flare of 6 November, 1980 in different X-ray lines of the SMM Flat Crystal Spectrometer and in the HXIS image (in X-rays above 3.5 keV), compared with the Hα loops. Time: 16:28 UT. (b) Time-variation of the measured altitude of the flare loops in Hα, in X-ray lines corresponding to different temperatures (cf. text), and in **HXIS** (or Fe XXV which yields very similar images). Two dashed lines follow the growth of the loop system at low temperatures (10^4 K in Hα and 2×10^6 K in O VIII) and at 10^7 K (Si XIII), respectively. Arrows and times indicate the cooling of stationary loops. The real cooling path of the shrinking loops is indicated for the Si XIII loop at 16:28 UT by the dotted curve. (After Švestka *et al.*, 1987.)

3.1.3. *Indirect Evidence for Reconnection*

With our present, limited spatial resolution, we do not have, and probably cannot have, any direct evidence of the reconnection process. But indirect evidence does exist:

Sakurai (1985), and before him Roy (1972), have shown that the loop-prominence systems of dynamic flares can be fit by potential-field modelling. In confined flares, according to Sakurai, potential-field modelling does not show any loops connecting the Hα footpoints or fitting the X-ray source. Thus the magnetic modelling indicates that the magnetic field structure is simplified in the case of a dynamic flare, possibly through reconnection of field lines which, prior to the field opening, were not potential.

Some 15 min after the maximum of the well-observed dynamic flare of 21 May, 1980 a new X-ray source appeared above the existing system of loops. This new source was first detected in the highest energy channels and only later on at lower energies (Švestka and Poletto, 1985). This indicates a source of small dimensions and high temperature in the corona.

Finally I may mention observations of post-flare loops made by Hanaoka, Kurokawa, and Saito (1986) during a solar eclipse. Their images indicated the existence of a cusp at the top of the loop system in the Fe XIV line, the hottest line they used.

3.2. Modifications of the Model

3.2.1. *Additional Heating*

It was definitely established more than two decades ago by Kleczek (1964) that the plasma condensations seen in the post-flare loops cannot originate in the corona: there is simply not enough coronal material available to provide this plasma. Thus, the material seen in the loops must evaporate from below, from the chromosphere, and it must be heated to the observed temperatures, close to 20×10^6 K at the top of the loops. The original Kopp and Pneuman model assumed that a gas-dynamic shock propagates downward from the reconnection site and heats the upflowing plasma to $3\text{–}4 \times 10^6$ K. But this is insufficient when compared with the loop temperatures observed. Six years later, Pneuman (1982) added to it the global Ohmic heating due to reconnection. This might have raised the temperature by about a factor of two, but it was still far from the values actually observed at the tops of the newly formed loops.

But there are other ways to enhance the heating. Cargill and Priest (1983) suggested heating of post-flare loops by slow MHD shocks. Figure 2 illustrates their idea: the rising *Y*-type neutral point trails behind a pair of slow shocks which heat the upflowing plasma and bring it to rest. Another way to enhance the energy release during the reconnection process in the Kopp and Pneuman model was considered by Somov and Titov (1985): they demonstrated that a small transverse component of magnetic field in a turbulent current sheet could increase the energy output by several orders of magnitude. Kopp and Poletto (1984) applied the reconnection model to the well observed and relatively simple spotless dynamic flare of 29 July, 1973 and found good agreement with several parameters of the growing loop system during its entire lifetime starting soon after the flare onset.

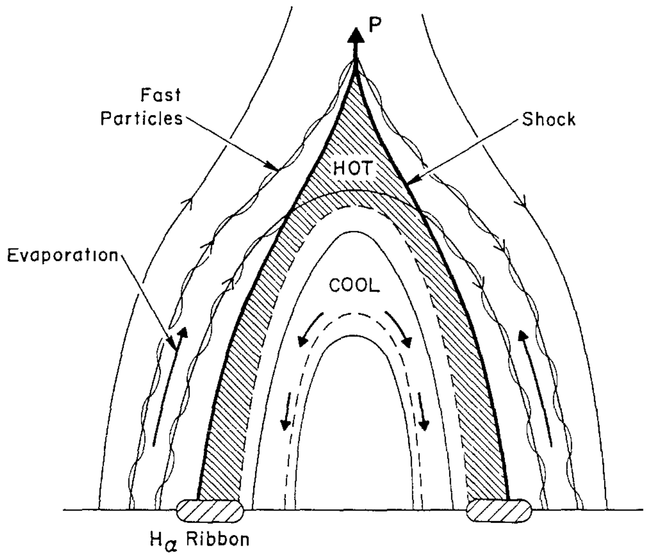

Fig. 2. The system of dynamic-flare loops some time after the reconnection has started. The neutral point P is rising vertically with decreasing velocity trailing behind it two slow MHD shocks (thick lines). These shocks heat the plasma which evaporates from the chromosphere. Behind the shocks is then a series of hot loops (shaded); the previously heated lower loops cool and one can eventually see the cooled material falling in Hα. (After Cargill and Priest, 1983.)

3.2.2. *Chromospheric Evaporation*

According to Kleczek (1964), between 10^{16} and 10^{17} g of material must be supplied to the top of post-flare loops during the gradual phase. Forbes and Priest (1983) have considered direct particle acceleration as the source of this upward flow, but ended with the result that an indirect, thermally-driven acceleration, such as ablation or evaporation, is necessarily needed. Again, in the original Kopp and Pneuman model the amount of evaporated material was only a fraction of that required, but there are ways to enhance it.

Forbes and Malherbe (1986) have shown that in addition to the slow-mode MHD shocks, considered by Cargill and Priest and shown in Figure 2, there also exists a fast-mode shock generated by the reconnection process. This fast shock can contribute to the chromospheric ablation and thus help to trigger a thermal condensation, that means a loop prominence, provided the reconnecting magnetic fields are sufficiently strong.

Indeed, Schmieder *et al.* (1987) found evidence for gentle chromospheric evaporation during the gradual phase of major dynamic flares (Figure 3(a)): in three flares studied, small blue shifts lasting for several hours were observed in the flare ribbons, which can be interpreted as upward chromospheric flows with speeds of 0.5–10 km s^{-1}. These upflows are sufficient to supply 10^{16} g or slightly more needed to maintain a dense ($n = 10^{12}$ cm^{-3}) Hα post-flare loop system in the corona. By contrast, the region between the two ribbons exhibits large red shifts that are typical for falling material in

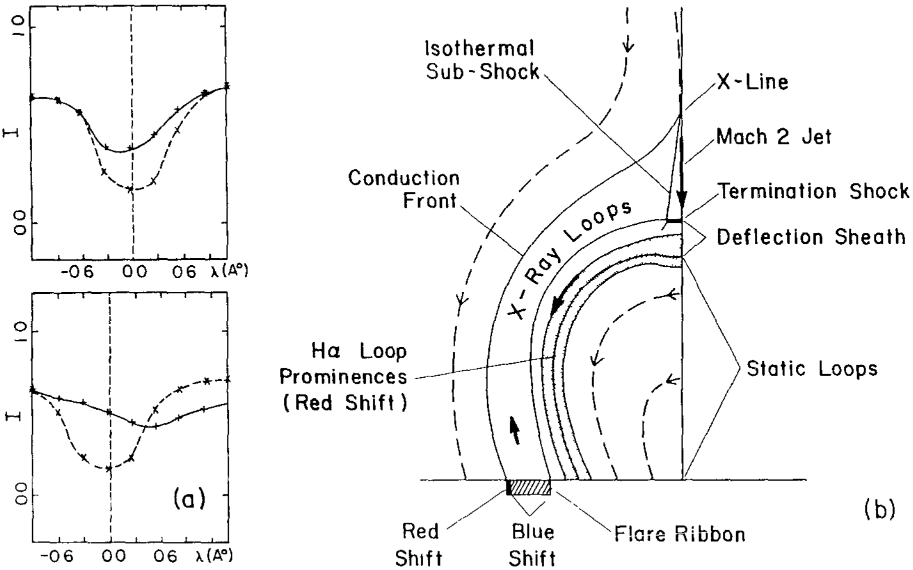

Fig. 3. (a) An example of observed Hα line profiles (solid lines) in the ribbons (*above*) and in the loops (*below*) of the dynamic flare of 16 May 1981. Dashed lines show the quiet-Sun reference profile. The blue shift in the ribbons corresponds to an upflow velocity of 4.5 km s^{-1}; the red shift in the loops corresponds to a downflow velocity of 24 km s^{-1} for optically thick, and 45 km s^{-1} for optically thin loops. (b) The inferred flow pattern for a reconnection model of the gradual phase (see text). (After Schmieder *et al.*, 1987.)

the cool Hα post-flare loops. The expected flow pattern is shown in Figure 3(b). In another analysis of chromospheric spectra of a dynamic flare by Wei-Qun and Cheng (1987) the authors deduced that about 9×10^{15} g of mass evaporated during the flare from the chromosphere to the corona.

One should realize that the density of 10^{12} cm^{-3} assumed by Schmieder *et al.* and also found in the study of the flare of 6 November, 1980, which I mentioned earlier (Figure 1), is the density in loops that, in projection on the solar disk, appeared in emission in the Hα line. Most post-flare loops seen on the disk are in absorption and their density is lower. For example, Shilova and Starkova (1987), who used Giovanelli's (1967) computations of hydrogen emission at various densities and temperatures, found the density in dark post-flare loops between 7×10^{10} and 10^{11} cm^{-3}.

The narrow red-shifted region at the outer edge of the Hα ribbon in Figure 3(b) can be explained as due to downward motion of the lower chromospheric level, which occurs when it is suddenly heated. MacNeice (1986) simulated the impact of a downward propagating coronal conduction front in a loop on the transition region and upper chromosphere. An accelerating upward moving ablation front and a downward moving compression is generated, just as the blue and red shifts in Figure 3 indicate.

The evaporation process has been studied by several authors, mainly by Canfield, Fisher, Gunkler, and their co-authors, but in most cases only evaporation during the impulsive phase has been considered. Fisher (1986) distinguishes two types of evaporation: an explosive one, if the chromosphere is heated by particle flows and the heating exceeds a certain threshold limit, and a non-explosive evaporation through conduction. The maximum upflow velocities during an explosive evaporation can reach 2.3 sound speeds as the maximum, whereas the non-explosive evaporation runs at speeds which are about 10 to 20% of this upper limit. During the gradual phase we encounter the lower speeds which generally agrees with Schmieder *et al.*'s values. A problem which still remains is the prevailance of radiative energy losses, demonstrated, e.g., by Doyle and Raymond (1984): a large fraction of the conducted flux is radiated away in the upper transition region so that the flux which eventually enters the upper chromosphere may be greatly reduced.

3.3. Shrinking of the Loops

Let me draw attention once again to Figure 1(a): altitudes of the loop tops imaged in various spectral lines. So far we have tacitly assumed that a loop is newly formed at a certain altitude in the corona and stays there; first it is heated, thus becoming visible in X-rays, and then it cools, becoming sequentially visible in cooler and cooler lines until it eventually appears in Hα. During the Skylab workshop, Moore *et al.* (1980) even determined the cooling times from the time difference between the appearance of a loop at a certain altitude in X-rays and in Hα.

However, a study of the event of 6 November, 1980 reveals that a loop does not stay at the altitude at which it was formed (Švestka *et al.*, 1987). We have made more such images like Figure 1(a) and compared the time variation of the altitude of the loop tops in different lines. This is shown on Figure 1(b). Let us consider the observation of Si XIII at 16:28 UT. If the loop we see here stayed at the same altitude while cooling, it would appear after 1 hr and 7 min in the Hα line. For pure radiative cooling, this cooling time corresponds to a density of 4×10^9 cm^{-3} (and less if conduction also contributes to the cooling process). However, the Hα loops were in emission, hence their density must be 10^{12} cm^{-3} or more. Such a dense loop would cool purely by radiation, and the cooling time from the Si XIII temperature would not exceed 2 min. The implication is that the density must be increasing during the life of the loop, and the loop cannot stay at a constant altitude, but must gradually shrink. The real cooling path would then be similar to the dotted curve in Figure 1(b).

The whole process is schematically shown in Figure 4: a magnetic reconnection produces a loop; energy input from the reconnection point then evaporates chromospheric plasma into the loop which gradually cools and shrinks: the resulting O VIII and Hα loops are at much lower altitude than where the loop had been originally formed. According to Kopp and An (private communications), the chromospheric evaporation should first lead to an expansion of the loop. However, if the loop becomes very dense, and thus very heavy, gravitational forces will cause the loop to collapse and seek a different equilibrium configuration at a lower altitude.

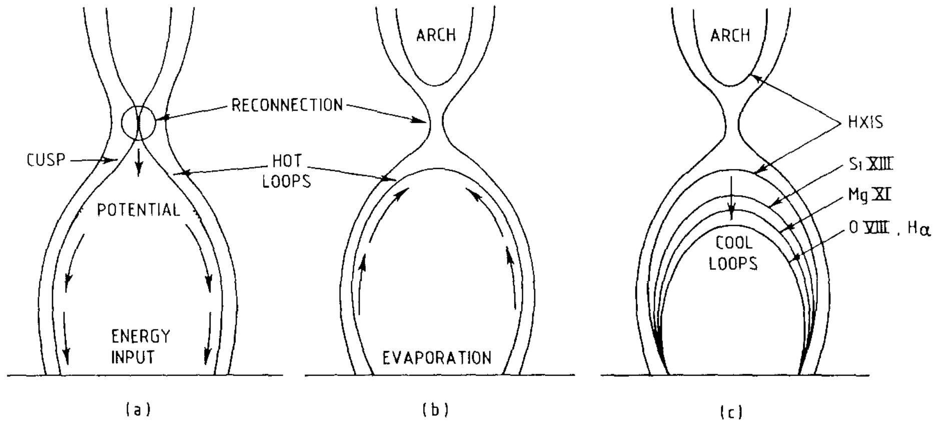

Fig. 4. A tentative scenario of the loop formation (a), heating (b), and cooling (c), based on the observations presented in Figure 1. (After Švestka *et al.*, 1987.)

3.4. Giant post-flare X-ray arches

The 'arch', shown in Figure 4, is the expected upper corona product of the reconnection process. I suppose that its discussion should be included in a review of the gradual phase, because, first, it may be considered as the gradual phase of a dynamic flare at very high coronal altitudes and, second, it is probably related to some other observations of the gradual phase which we will discuss in the next section.

The first arch of this kind was detected by HXIS in 4 keV X-rays on 22 May, 1980 (Švestka *et al.*, 1982a): the associated flare appeared at 21:00 the day before, and the arch could be seen until 08 UT the next day, i.e., for 11 hours after the flare onset. During the same period Culgoora observed a stationary type I noise storm above the site of the arch. The flare of 6 November, to which Figures 1 and 4 refer, was associated with another arch (Švestka *et al.*, 1982b). Again, Culgoora observed type IV continuum above the source on the day of the flare, and a type I noise storm the day after. Figure 5 shows the time development of the arch in soft X-rays; the lower traces on the graph show the time development of emission mensure and temperature. The temperature peaks first, after approximately one hour, the flux peaks second, and the emission measure last, 3.5 hours after the flare onset. This is, as under a magnifying glass, the same development we see low in the solar atmosphere in flares. Thus the arch really may be considered as the gradual phase of the dynamic flare at the altitude of some 100 000 km in the corona.

Švestka *et al.* (1982a) have suggested that such an arch is the upper product of the reconnection process during dynamic flares. After the reconnection, the originally sheared field lines produce much less sheared (quasi-potential, remember Sakurai's (1985) modelling) post-flare loops below and the arch structure above. Though these arches are created by some dynamic flares, their magnetic configuration then apparently persists in the corona, because when another dynamic flare appears, essentially the same structure reappears again in soft X-rays (Švestka, 1984).

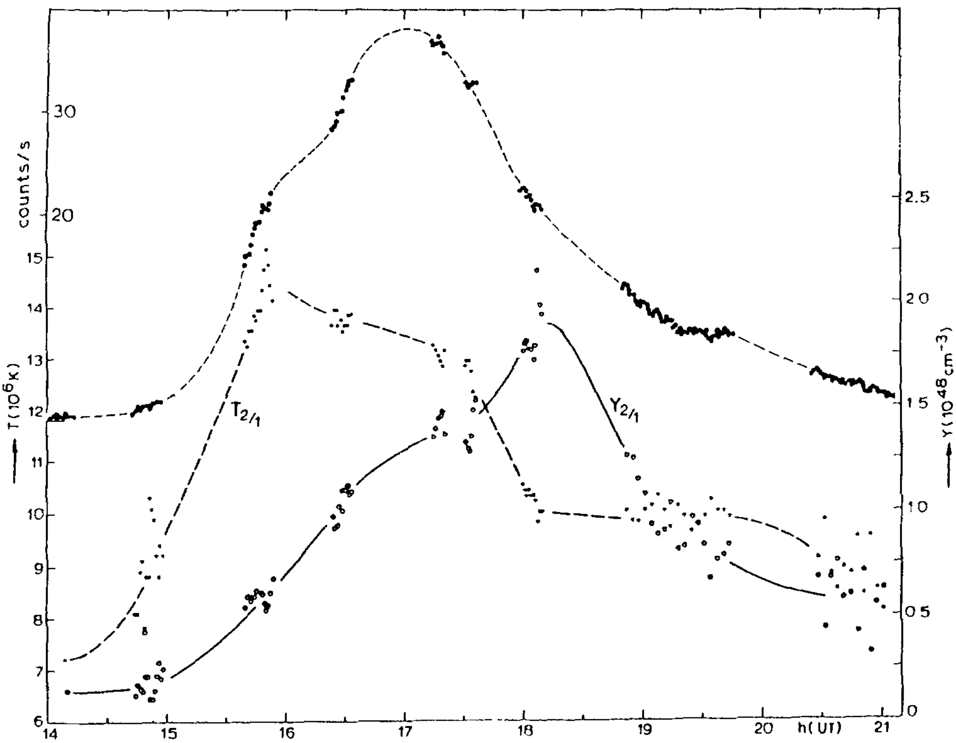

Fig. 5. Time development of the giant post-flare arch that followed the dynamic flare of 14:44 UT on 6 November, 1980 (tentatively the 'arch' of Figure 4). All curves refer to an average altitude of 100000 km. The upper curve shows the number of counts in 3.5–5.5 keV X-rays, the lower ones the temperature ($T_{2/1}$; left scale) and emission measure ($Y_{2/1}$; right scale). (After Švestka, 1984.)

3.5. Radio type IV events and noise storms

Similar structures were actually seen long ago on radio waves. As early as 1961 Pick showed that metric type IV bursts, which as we know are associated with dynamic flares, consist of two parts: the first part sets in at the onset of the flare and the second part later on, during the first-part decay. In November 1968 Wild (1969) imaged at 80 MHz the radio event shown in Figure 6. The components *A*, *B*, *C* are components of a moving type IV burst and correspond to the first part. The component *D* is a stationary burst located above the site of the flare (the cross) and corresponds to the second part. There is little doubt that what Wild observed here as the source *D* is the same structure which HXIS observed as the arch in X-rays.

Klein *et al.* (1983) have found that the first part (the moving type IV) is associated with hard X-rays; in the second part the hard X-rays are missing, but the burst is associated with soft X-ray emission. Klein *et al.* conclude that during this second phase the energy release is less efficient, but still continues, and that the simultaneous occurrence of X-rays and metric type IV indicates existence of large-scale magnetic arches.

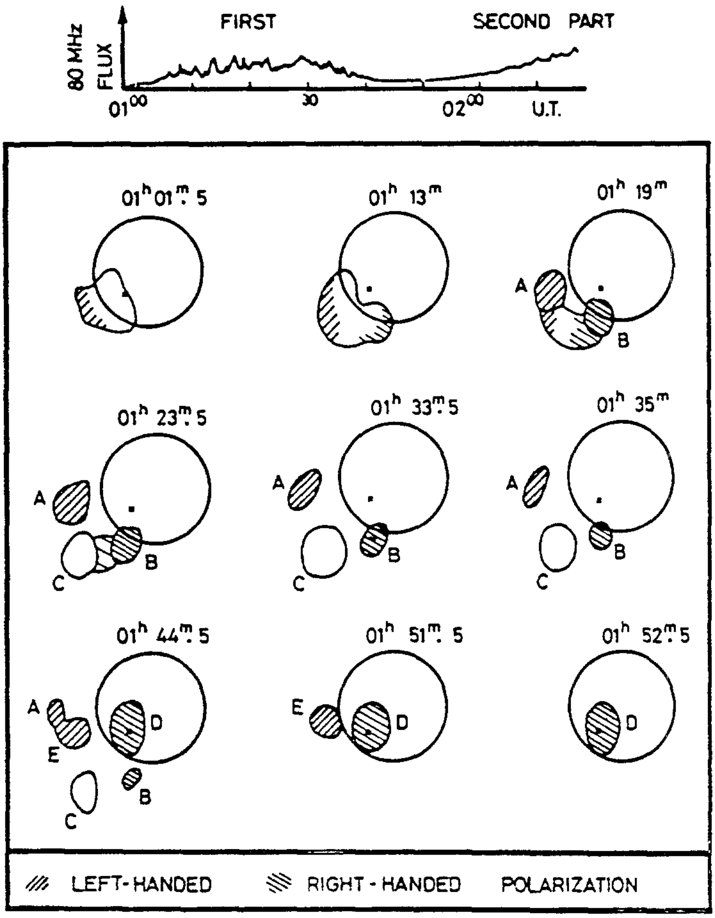

Fig. 6. Sources of the type IV burst on 22 November, 1968, as recorded by the 80 MHz radioheliograph at Culgoora. Position of the associated flare is marked with a cross. *Above*: record of the integrated 80 MHz flux showing the two parts of the type IV, corresponding to the moving (A, B, C) and stationary (D) sources, respectively. (After Wild, 1969.)

In another study Kai *et al.* (1986) observed in several dynamic flares delayed bursts which appeared 0.5 to 1 hour after the strong impulsive-phase bursts had faded. These delayed bursts were observed from microwaves to meter waves. The authors concluded that electrons were accelerated to the range of MeV even tens of minutes after the impulsive phase acceleration had ceased. The wide difference in wavelengths at which this delayed radio bursts appeared is again evidence that the delayed energy release occurs in a giant magnetic structure extending to at least 200 000 km altitude, and that is also the altitude where we see the tops of X-ray post-flare arches.

An intriguing problem, associated with long-lasting post-flare bursts is the hardening of the X-ray spectrum in some of them. Several such events were observed by Hinotori (e.g., Takakura *et al.*, 1984) and by the Hard X-Ray Burst Spectrometer on the SMM (e.g., Cliver *et al.*, 1986). Takakura *et al.* observed three successive peaks in a flare event which became progressively harder. Cliver *et al.* observed flare events in which the spectral index γ was decreasing with time. Figure 7 shows an example in which γ was steadily decreasing for more than 40 minutes. In one of similar sources, Vilmer, Kane, and Trottet (1982) estimated its density to at least 10^{10} cm^{-3}. In another case, when such a source was imaged close to the limb, its altitude could be estimated at 40000 km and it did not change its position (during 14 min of imaging with spatial resolution of about 15 arc sec; Tsuneta *et al.*, 1984). Thus again these are stationary or very slowly moving bursts which are somehow connected with the tops of the newly formed loops below the post-flare arch.

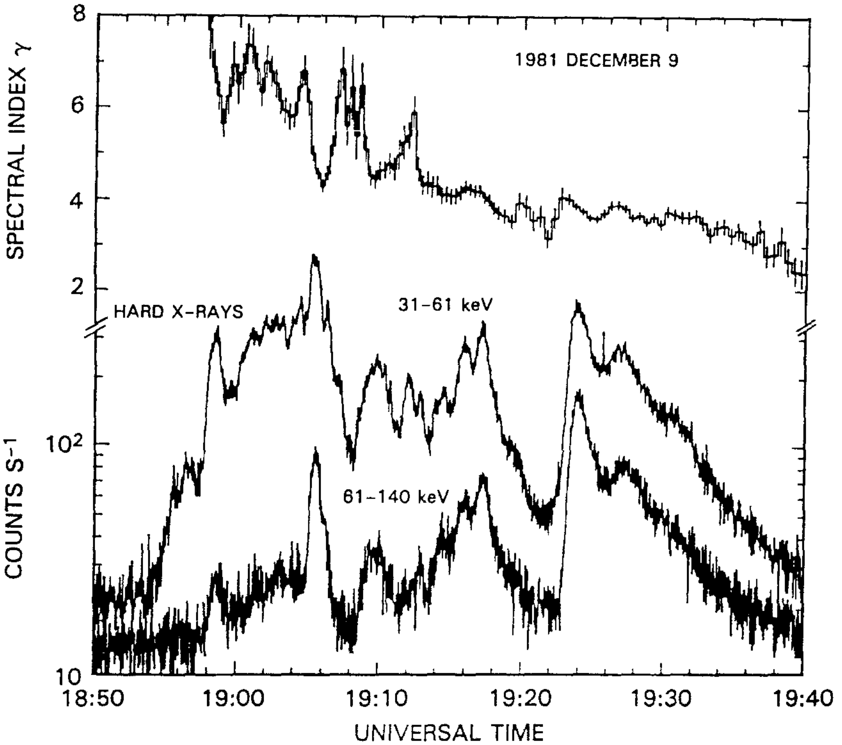

Fig. 7. Hard X-ray time profiles (31–61 keV and 61–140 keV) of the dynamic flare on 9 December, 1981. The uppermost curve shows the gradual decrease of the spectral index γ, relatively unaffected by variations in the X-ray flux. (After Cliver *et al.*, 1986.)

As Cliver *et al.* (1986) have pointed out, there is multiple evidence that sources of this hard X-ray radiation are significantly higher than the sources we see during the impulsive phase: (1) There are very small related changes in Hα; (2) the frequency of maximum radio flux is low (which implies low magnetic field strength); and (3) the bursts are microwave rich; this implies less bremsstrahlung, i.e., low density. Tsuneta (1983) has interpreted the systematic hardening in terms of the energy-dependent collisional loss of electrons confined in a magnetic trap. Trapping, alone, however, without prolonged acceleration, in insufficient to account for the observed degree of spectral hardening, as Bai and Dennis (1845) pointed out.

3.6. Complex structures of dynamic flares

Gopalswamy and Kundu (1987) have demonstrated how extremely diverse the positions of different radio bursts can be above a dynamic flare site. In the flare they studied, the various continua observed before, during, and after the flare were at different positions and altitudes, probably due to electron trapping in different arches. The type II burst, i.e., the flare-associated shock, moved in a completely separate direction. This is a particularly interesting observation, because it may explain why we sometimes see both the mass ejection associated with a dynamic flare and a quasi-stationary arch above the flare site.

Indeed, some dynamic flares may be extremely complex phenomena. Apart from the common two-ribbon flares, there are also three-ribbon and four-ribbon flares (cf. Tang, 1985). Ogir and Antalová (1986) suggested that a three-ribbon flare is a misleading image of two chromospheric ribbons and projected bright tops of the loops, but that, according to Tang, is not always the case. The third ribbon may really represent a complex structure of loops, like in the case shown in Figure 8, after Kundu, Schmahl, and Velusamy (1982). A four-ribbon flare is still more complex. Besides, one may encounter quite anomalous cases, like the 'circular two-ribbon flare' presented in her paper by Tang (1985).

3.7. Small dynamic flares

Tang (1985) has found in many small flares that what looks like ribbons in them does not usually show any measurable separation of the chromospheric bright structures. Therefore, these events are probably confined flare arcades. But some small flares do show the ribbon expansion which implies that not all dynamic flares are big long-duration events.

This seems to be confirmed by a study made by Lin, Lin, and Kane (1985). From an analysis of flares observed by ISEE-3 they deduced that in 40% of cases there are two components during the decay phase of solar flares: a usual flare plasma at about 10 million degrees, cooling, and a superhot one, with temperature of at least 30 million

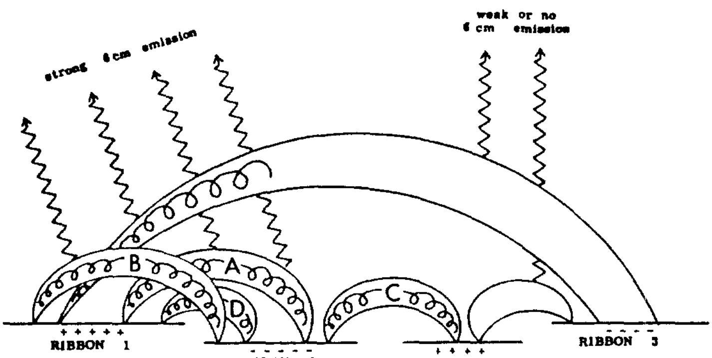

Fig. 8. Sketch of the magnetic field structure of a three-ribbon flare on 25 June, 1980 deduced from radio, Hα, and magnetogram data. (After Kundu, Schmahl, and Velusamy, 1982.)

degrees, which requires an additional input of energy after the impulsive phase. In Figure 9 the right-hand flare event belongs to this category while the left-hand event does not: there a two-temperature fit does not produce any improvement. Note that the right-hand event, though moderately small and relatively short-lived, still has a more gradual time profile than the other one. Thus one can suppose that this was a relatively small dynamic flare, with continued release of energy in the late phase, whereas the left-hand event was a confined flare, with all energy released during the impulsive phase. Several other examples can be found in the paper by Lin, Lin and Kane.

4. Flare Hybrids

Some flares, however, are quite clearly hybrids of the two classes we discussed before. That dynamic flare to which Figures 1, 4, and 5 are related, on 6 November, 1980, started at 14:44 UT as a confined flare and the dynamic-flare loops began to develop only tens of minutes later. Harrison *et al.* (1983) presented an example of another flare, on 5 July, 1980, which started as a compact flare. De Jager (private communication) is

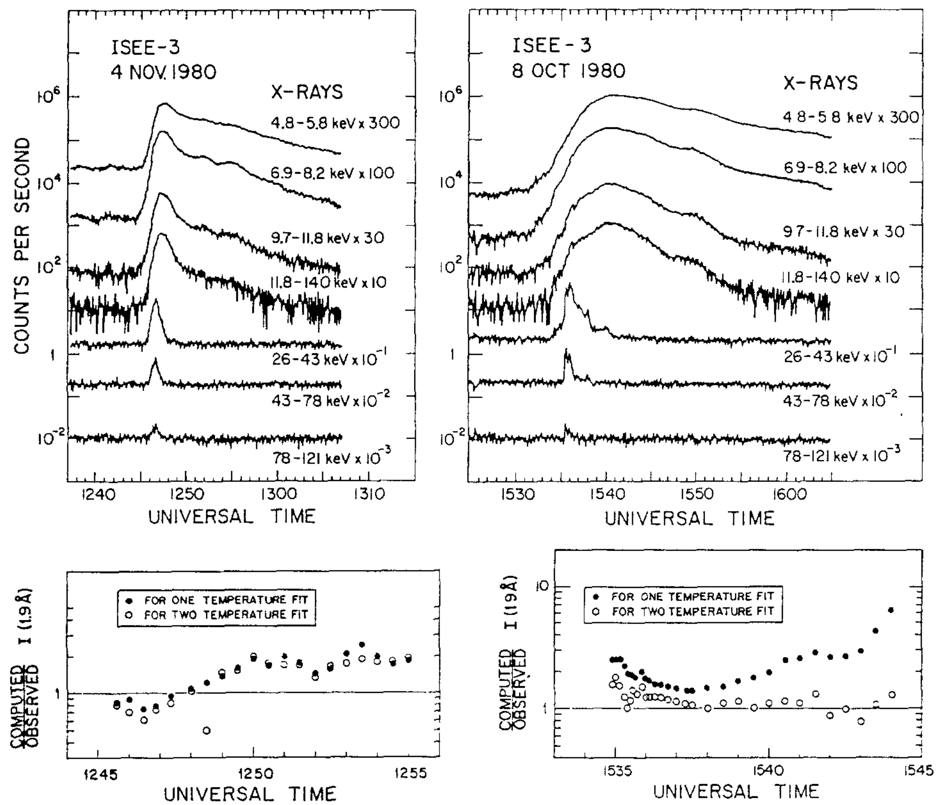

Fig. 9. The X-ray counting rate versus time profiles (*above*) and results of fitting procedure for one-temperature and two-temperature fit (*below*) for a tentatively confined (*left*) and dynamic (*right*) flare. (Examples taken from Lin, Lin, and Kane, 1985.)

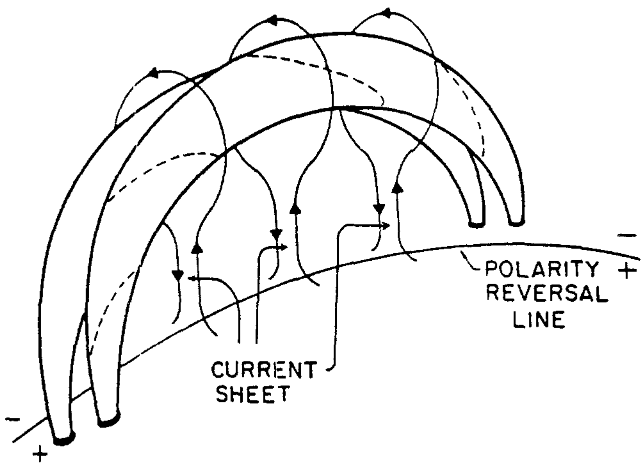

Fig. 10. Schematic representation of the development of an extended current sheet beneath an erupting filament. (After Sturrock *et al.*, 1984.)

of the opinion that quite often (and possibly always) a compact flare may serve as a trigger for a dynamic flare; we do not know, actually, what causes the magnetic field to open and thus start the dynamic flare process.

Sturrock *et al.* (1984) have suggested that the onset phase of a two-ribbon dynamic flare may be due to reconnection of contiguous but oppositely directed magnetic flux tubes linking a filament to the photosphere (Figure 10). A set of reconnections below the filament causes its eruption and starts the flare. Until the filament erupts and the field opens, and before the open field lines begin to reconnect, the set of reconnections in the configuration of Figure 10 clearly can simulate the character of a confined flare.

As a matter of fact, there are still relatively few flares for which good images at different wavelengths (X-rays, UV, optical, radio) are available. In the set of high-resolution Hα data at the Big Bear Observatory, for example, one finds many strange events, for which the classification is extremely difficult when no images of the coronal X-ray or radio flare are available. Some flares seem to be hybrids of the two classes, some others are either confined or dynamic flares accompanied by other associated phenomena (surges, sprays, flaring arches, or loop connections of which only the remote footpoints become visible in Hα). In the same way, the Hinotori flare classification (cf., e.g., Dennis, 1985) which is based solely on X-ray images with poor spatial resolution, encounters many hybrids and events for which the classification is questionable. Hopefully, the rising solar cycle will provide more complete and more coordinated flare observations which will help us to understand better all these varieties in the flaring plasma configuration.

References

Acton, L. W., Canfield, R. C., Gunkler, T. A., Hudson, H. S., Kiplinger, A. L., and Leibacher, J. W.: 1982, *Astrophys. J.* **263**, 409.

Antiochos, S. K. and Sturrock, P. A.: 1978, *Astrophys. J.* **220**, 1137.
Antiochos, S. K. and Sturrock, P. A.: 1982, *Astrophys. J.* **254**, 343.
Bai, T. and Dennis, B. R.: 1985, *Astrophys. J.* **292**, 699.
Bruzek, A.: 1969, in C. de Jager and Z. Švestka (eds.), *Solar Flares and Space Research*, North-Holland, Amsterdam, p. 61.
Cargill, P. J. and Priest, E. R.: 1983, *Astrophys. J.* **266**, 383.
Cliver, E. W., Dennis, B. R., Kiplinger, A. L., Kane, S. R., Neidig, D. F., Sheeley, N. R., and Koomen, M. J.: 1986, *Astrophys. J.* **305**, 920.
De Jager, C., Machado, M. E., Schadee, A., Strong, K. T., Švestka, Z., Woodgate, B. E., and van Tend, W.: 1983, *Solar Phys.* **84**, 205.
Dennis, B. R.: 1985, *Solar Phys.* **100**, 465.
Doyle, J. G. and Raymond, J. C.: 1984, *Solar Phys.* **90**, 97.
Fisher, G. H.: 1986, in D. Mihalas and K. H. Winkler (eds.), 'Radiation Hydrodynamics in Solar Flares', *Lecture Notes in Physics* **255**, 53.
Forbes, T. G. and Malherbe, J. M.: 1986, *Astrophys. J.* **302**, L67.
Forbes, T. G. and Priest, E. R.: 1983, *Solar Phys.* **88**, 211.
Giovanelli, R. G.: 1967, *Australian J. Phys.* **20**, 81.
Gopalswamy, N. and Kundu, M. R.: 1987, *Solar Phys.* **111**, 347.
Hanaoka, Y., Kurokawa, H., and Saito, S.: 1986, *Solar Phys.* **105**, 133.
Harrison, R. A., Simnett, G. M., Hoyng, P., Lafleur, H., and van Beek, H. F.: 1983, *Solar Phys.* **84**, 237.
Heinzel, P. and Karlický, M.: 1987, *Solar Phys.* **110**, 343.
Kahler, S. W.: 1977, *Astrophys. J.* **214**, 891.
Kai, K., Nakajima, H., Kosugi, T., Stewart, R. T., Nelson, G. J., and Kane, S. R.: 1986, *Solar Phys.* **105**, 383.
Kleczek, J.: 1964, in *AAS-NASA Symp. on Physics of Solar Flares*, NASA, Washington, D.C., p. 77.
Klein, L., Anderson, K., Pick, M., Trottet, G., Vilmer, N., and Kane, S.: 1983, *Solar Phys.* **84**, 295.
Kopp, R. A. and Pneuman, G. W.: 1976, *Solar Phys.* **50**, 85.
Kopp, R. A. and Poletto, G.: 1984, *Solar Phys.* **93**, 351.
Kundu, M. R., Schmahl, E. J., and Velusamy, T.: 1982, *Astrophys. J.* **253**, 963.
Lin, H. A., Lin, R. P., and Kane, S. R.: 1985, *Solar Phys.* **99**, 263.
MacCombie, W. J. and Rust, D. M.: 1979, *Solar Phys.* **61**, 69.
Machado, M. E.: 1987, *Solar Phys.* **113**, 57.
MacNeice, P.: 1986, *Solar Phys.* **103**, 47.
Martin, S. F. and Švestka, Z. F.: 1988, *Solar Phys.* **116**, 91.
Moore, R., McKenzie, D. L., Švestka, Z., Widing, K. G., and 12 co-authors: 1980, in P. A. Sturrock (ed.), *Solar Flares*, Colorado Associted University Press, p. 341.
Mouradian, Z., Martres, M. J., and Soru-Escaut, I.: 1983, *Solar Phys.* **87**, 309.
Ogir, M. B. and Antalová, A.: 1986, *Bull. Astron. Inst. Czech.* **37**, 344.
Pallavicini, R., Serio, S., and Vaiana, G. S.: 1977, *Astrophys. J.* **216**, 108.
Pallavicini, R., Peres, G., Serio, S., Vaiana, G., Acton, L., Leibacher, J., and Rosner, R.: 1983, *Astrophys. J.* **270**, 270.
Petrasso, R. D. and Krieger, A. S.: 1976, *Solar Phys.* **47**, 167.
Petrasso, R. D., Kahler, S. W., Krieger, A. S., Silk, J. K., and Vaiana, G. S.: 1975, *Astrophys. J.* **199**, L127.
Pick, M.: 1961, *Ann. Astrophys.* **24**, 183.
Pneuman, G. W.: 1982, *Solar Phys.* **78**, 229.
Roy, J. R.: 1972, *Solar Phys.* **26**, 418.
Rust, D. M., Simnett, G. M., and Smith, D. F.: 1985, *Astrophys. J.* **288**, 401.
Sakurai, T.: 1985, *Solar Phys.* **95**, 311.
Schmahl, E. J., Kundu, M. R., and Erskine, F. T.: 1986, *Solar Phys.* **105**, 87.
Schmieder, B., Forbes, T. G., Malherbe, J. M., and Machado, M. E.: 1987, *Astrophys. J.* **317**, 956.
Shilova, N. S. and Starkova, L. I.: 1987, *Kinematika i fizika nebeskich tel 3*, No. 6, 28.
Somov, B. V. and Titov, V. S.: 1985, *Solar Phys.* **102**, 79.
Sotirovski, P , Simon, G., and Rust, D. M.: 1986, in D. F. Neidig (ed.), *The Lower Atmosphere of Solar Flares*, National Solar Observatory, Sunspot, New Mexico, p. 71.
Sturrock, P. A.: 1968, in K. O. Kiepenheuer (ed.), 'Structure and Development of Solar Active Regions', *IAU Symp.* **35**, 471.

Sturrock, P., Kaufman, P., Moore, R. L., and Smith, D. F.: 1984, *Solar Phys.* **94**, 341.
Švestka, Z.: 1984, *Solar Phys.* **94**, 171.
Švestka, Z and Poletto, G.: 1985, *Solar Phys.* **97**, 113.
Švestka, Z., Stewart, R., Hoyng, P., Van Tend, W., Acton, L. W., Gabriel, A. H., Rapley, C. G., and 8 co-authors: 1982a, *Solar Phys.* **75**, 305.
Švestka, Z., Dennis, B. R., Pick, M., Raoult, A., Rapley, C. G., Stewart, R. T., and Woodgate, B. E.: 1982b, *Solar Phys.* **80**, 143.
Švestka, Z. F., Fontenla, J. M., Machado, M. E., Martin, S. F., Neidig, D. F., and Poletto, G.: 1987, *Solar Phys.* **108**, 237.
Takakura, T., Ohki, K., Sakurai, T., Wang, J. L., Xuan, J. Y., Li, S. C., and Zhao, R. Y.: 1984, *Solar Phys.* **94**, 359.
Tang, F.: 1985, *Solar Phys.* **102**, 131.
Tsuneta, S.: 1983, Thesis, University of Tokyo.
Tsuneta, S.: 1987, *Solar Phys.* **113**, 35.
Tsuneta, S. Takakura, T., Nitta, N., Ohki, K., Tanaka, K., Makishima, K., Murakami, T., Oda, M., Ogawara, Y., and Kondo, I.: 1984, *Astrophys. J.* **280**, 887.
Van Hoven, G.: 1981, in E. R. Priest (ed.), *Solar Flare Magnetohydrodynamics*, Gordon and Breach, New York, p. 217.
Vilmer, N., Kane, S. R., and Trottet, G.: 1982, *Astron. Astrophys.* **108**, 306.
Wei-Qun, G. and Cheng, F.: 1987, *Solar Phys.* **107**, 311.
Wild, J. P.: 1969, *Solar Phys.* **9**, 260.